

# Pulse energy scaling to 5 $\mu\text{J}$ from a femtosecond thin disk laser

Sergio V. Marchese, Thomas Südmeyer, Matthias Golling, Rachel Grange, and Ursula Keller

*Department of Physics, Institute of Quantum Electronics, ETH Zurich, 8093 Zurich, Switzerland*

Received April 26, 2006; revised June 28, 2006; accepted June 29, 2006;  
 posted June 30, 2006 (Doc. ID 70310); published August 25, 2006

We report an increase in pulse energy to 5.1  $\mu\text{J}$  obtained directly from a femtosecond diode-pumped Yb:YAG thin disk laser without external amplification. Stable passive mode locking was obtained with a semiconductor saturable absorber mirror (SESAM). The laser delivers 63 W of average output power in a nearly diffraction-limited beam ( $M^2=1.1$ ) at a center wavelength of 1030 nm. The pulse repetition rate is 12.3 MHz, and the pulses have a duration of 800 fs, which results in a peak power of 5.6 MW. The laser was operated in a box flooded with helium because the nonlinearity of air was found to be a limiting factor for the stability of the pulse formation at increasing pulse energies. © 2006 Optical Society of America  
 OCIS codes: 140.3480, 140.3580, 140.4050.

The average power of femtosecond thin disk lasers has continually increased in recent years. Pulse energies beyond the microjoule level have been obtained with average powers of up to 80 W.<sup>1,2</sup> The high peak power in the megawatt regime makes these lasers suitable for direct pumping of high-gain parametric devices<sup>3–6</sup> for large-scale red–green–blue laser projection systems.<sup>2</sup> With pulse energies entering the 1–10  $\mu\text{J}$  regime, these lasers also become more interesting for material processing applications without further amplification. So far, the highest pulse energy obtained directly from a femtosecond thin disk laser was 1.75  $\mu\text{J}$ .<sup>1</sup> Similar pulse energies at high repetition rates can also be generated by using a fiber-based chirped-pulse amplification system based on a mode-locked seed oscillator and two fiber amplifier stages.<sup>7</sup> Alternatively, very long cavity oscillators<sup>8–10</sup> and cavity dumping<sup>11</sup> were used to increase the pulse energy directly obtained from femtosecond laser oscillators, and with cavity dumping a pulse energy of 1.35  $\mu\text{J}$  in femtosecond pulses was obtained. Owing to the low average power of the lasers used in these two approaches, the repetition rates need to be significantly reduced when high pulse energies are desired.

In this Letter we demonstrate a passively mode-locked Yb:YAG thin disk laser that delivers pulses with an energy of 5.1  $\mu\text{J}$ . This significant increase in pulse energy over previous results was made possible by realizing the importance of the nonlinearity of air inside a thin disk laser cavity, which adds to the total Kerr nonlinearity and is responsible for the instabilities that previously limited further pulse energy scaling.<sup>1</sup>

In a thin disk laser, the gain is provided by a laser material with a thickness much smaller than the spot diameter of the pump and laser mode.<sup>12</sup> One face of the disk is coated for high reflectivity and directly attached to a heat sink. The disk is then used in reflection for both the pump and the laser beam. This special geometry allows fundamental transverse mode operation up to very high average powers, thanks to a nearly one-dimensional heat flow taking place longitudinally with respect to the beam axis. The generation of stable femtosecond pulses with a

SESAM<sup>13,14</sup> is realized by using soliton mode locking,<sup>15</sup> where the balanced effects of self-phase modulation (SPM) and negative group-delay dispersion (GDD) lead to the formation of solitonlike pulses. The thin disk does not significantly contribute to the nonlinearity because of its small thickness and the large mode radius of the laser beam. Therefore the SPM is typically introduced by a glass plate positioned in the beam. The GDD is introduced by a set of dispersive mirrors. Similar to the thin disk, the SESAM is operated with a spot size larger than the thickness of the substrate, and therefore efficient heat removal also takes place longitudinal to the beam axis. The first reported laser based on this concept was an Yb:YAG laser delivering 16 W of average output power in 730 fs pulses with a pulse energy of 0.47  $\mu\text{J}$ .<sup>16</sup> The average power was later scaled up to 60 W by taking advantage of the power scalability of the concept.<sup>1</sup> The pulse energy was scaled to 1.75  $\mu\text{J}$ . More energy scaling, however, was limited by strong nonlinearities of unknown origin that could not be compensated for with the available negative GDD. These nonlinearities led to unstable behavior and pulse breakup as well as regimes of stable operation with multiple pulses simultaneously oscillating inside the laser cavity. It was thus possible to achieve a higher average power of 80 W only by increasing the repetition rate to 57 MHz, which in return reduced the pulse energy to 1.4  $\mu\text{J}$ .<sup>2</sup>

The experimental setup of the laser presented here is shown in Fig. 1. The thin disk laser head is placed as a folding mirror inside a standing-wave cavity. As the gain medium we use an Yb:YAG crystal, which has a thickness of 200  $\mu\text{m}$  and is slightly wedged to eliminate residual reflections. An area with a 2.7 mm diameter is pumped with up to 230 W of average power at 940 nm from a fiber-coupled laser diode stack. For efficient absorption of the pump light, the pump optics are aligned for 24 passes through the disk.<sup>17</sup> Passive mode locking is achieved by inserting a SESAM as an end mirror into the laser cavity. The InGaAs SESAM has a saturation fluence of  $\approx 110 \mu\text{J}/\text{cm}^2$ , a modulation depth of  $\approx 0.5\%$  and low nonsaturable losses of  $< 0.1\%$ . Eight dispersive mir-

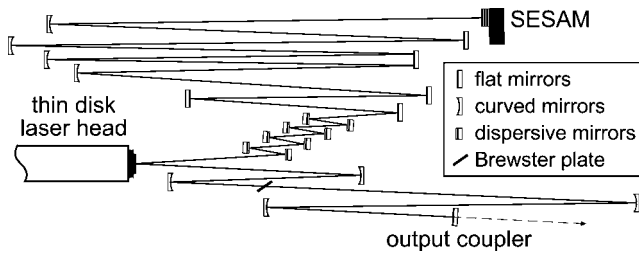


Fig. 1. Experimental setup of the Yb:YAG thin disk laser cavity (not to scale) with a length of 12.2 m, resulting in a repetition rate of 12.3 MHz. Eight dispersive mirrors introduce a total GDD of  $-8800 \text{ fs}^2$  per cavity round trip. The Brewster plate has a thickness of 1 mm.

rors with a GDD of  $-550 \text{ fs}^2$  each are used to introduce a total GDD of  $-8800 \text{ fs}^2$  per cavity round trip. A 1 mm thick fused silica plate is inserted at Brewster's angle to ensure linear polarization of the laser output and to provide the necessary Kerr nonlinearity for soliton mode locking. By shifting the plate's position along the beam propagation axis, the intensity and thus the nonlinear phase shift can be changed. As demonstrated in Refs. 15 and 18, this makes the pulse duration tunable. The laser was initially built with a length of 3.69 m, resulting in a repetition rate of 40.7 MHz. The thermal lens of the gain medium has an estimated focal length of  $-2.8 \text{ m}$ , and the resonator design was first optimized for best performance under these conditions. The cavity length was then increased by using simple  $4f$  extensions, each of which consists of two mirrors spaced by their equal radius of curvature  $R=2f$ , thus adding a total of  $2R$  to the cavity length. Propagation through such a  $4f$  imaging system results in a unity transformation for the  $q$  parameter of a Gaussian beam. Reducing the repetition rate with this approach does therefore not change the optimum operation point of the laser. We gradually decreased the repetition rate to 29.1, 16.5, and finally 12.3 MHz by using mirrors with an  $R$  of 750, 1500, and 2000 mm to extend the cavity to a final length of 12.2 m. Given the high output coupler transmission of 10%, additional losses introduced by these extensions did not significantly influence the performance of the laser. We estimate the total intracavity losses, not including output coupling, to be  $<4\%$ .

In this configuration the laser started stable mode locking at an average output power of 5 W when operated in an air atmosphere. However, the average power could be increased to only  $\approx 7 \text{ W}$  before instabilities were observed. A further increase resulted in multiple pulses simultaneously oscillating inside the laser cavity. This could be observed with our autocorrelator because these pulses were typically separated by only a few picoseconds. The operation of the laser appeared as equally stable as when operating with just one pulse oscillating in the laser cavity. Even in the regime of single-pulse operation, the pulse duration was only slightly affected by the amount of nonlinearity introduced by the Brewster plate. This suggests that we have soliton pulses oscillating inside the cavity with the presence of a significant Kerr

nonlinearity, which stems from a source other than the Brewster plate. These observations are similar to the ones made in Ref. 1 at a higher repetition rate. We found that this additional nonlinearity stems from the air atmosphere inside the laser cavity. Its contribution became more dominant as we increased the cavity length. Numerical estimations using the nonlinear refractive index of air<sup>19</sup> ( $\approx 4 \times 10^{-19} \text{ cm}^2/\text{W}$  at 800 nm) show good agreement with the missing nonlinearity in Ref. 1. To eliminate the air's contribution to the nonlinearity, we covered the entire laser with a box that was flooded with helium, which has a negligible nonlinearity compared with air.<sup>19</sup>

With the laser operating in a helium atmosphere, we were able to obtain stable mode-locked operation with an average power of up to 63 W, limited by the amount of available pump power. The pulses have a duration of 800 fs and a full width at half-maximum (FWHM) spectral bandwidth of 1.59 nm at a center wavelength of 1030 nm (Fig. 2), resulting in a time-bandwidth product of 0.36, which is only slightly larger than the ideal value for soliton pulses (0.315). With the pulse repetition rate of 12.3 MHz, the pulse energy is  $5.1 \mu\text{J}$  and the peak power is 5.6 MW. The beam quality is nearly diffraction limited with a measured  $M^2$  value of 1.1. The calculated beam radius on the SESAM is  $880 \mu\text{m}$ , leading to a saturation parameter of  $S \approx 19$ . Despite the large intracavity pulse energy of more than  $50 \mu\text{J}$ , we did not observe any damage of the SESAM or any other component of the laser. We could clearly observe a correlation between the nonlinearity and the helium content in the laser cavity. Because the box was not perfectly airtight, interrupting the helium supply for several seconds caused the air content and thus the nonlinearity inside the cavity to increase. The pulses consequently became shorter, in agreement with the soliton mode locking theory. Finally, the laser became unstable when the nonlinearity became too high. This effect was reversible: the laser went back into stable operation after the helium supply was restarted. Rather than flooding the entire laser cavity with helium, one

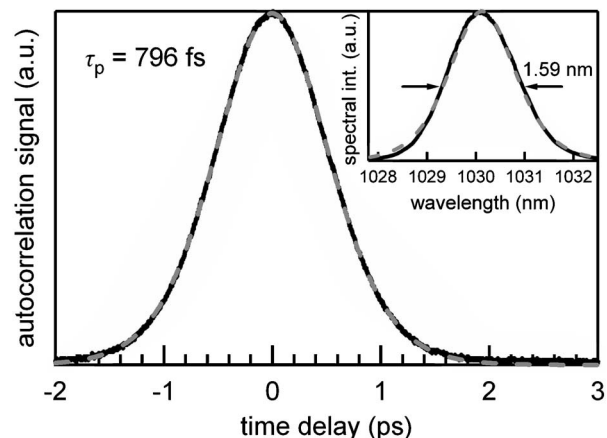


Fig. 2. Autocorrelation and (inset) optical spectrum of the measured output pulses. The dashed curves represent fitted curves with an ideal  $\text{sech}^2$ -shaped pulse of 796 fs duration and an optical bandwidth of 1.59 nm.

could consider using only a partial housing in the parts of the cavity where the intensities are the highest. Such an approach would simplify the task of building a helium-tight container. Besides helium flooding, lowering the pressure inside this container could then also be used to reduce the Kerr nonlinearity inside the laser cavity.

To confirm single-pulse operation, we traced the pulse train by using a fast sampling oscilloscope and a long-range autocorrelator. In addition, we measured the efficiency of second-harmonic generation (SHG) in a critically phase-matched 5 mm long  $\text{LiB}_3\text{O}_5$  crystal. This measurement was done in the regime of low conversion efficiency, with the output beam of the laser attenuated to a few watts. In this regime the generation of the second harmonic gives a good indication for single-pulse operation, because the conversion efficiency is significantly lower in the case of multiple pulsing owing to the reduced peak power. The measured data agreed well with numerical simulations for single-pulse operation and also with measurements done with the laser operating at low average power in an air atmosphere. Even though the setup was not optimized for maximum SHG efficiency, we obtained 30 W of average power at 515 nm when pumping with 57 W of pump power. This corresponds to a pulse energy of  $2.4 \mu\text{J}$  in the green.

In conclusion, we obtained  $5.1 \mu\text{J}$  pulses with a duration of 800 fs from a passively mode-locked Yb:YAG thin disk laser and an unoptimized SHG pulse energy of  $2.4 \mu\text{J}$ . The average output power is 63 W, and the output is nearly diffraction limited with an  $M^2$  value of 1.1. The increase in pulse energy was made possible by identifying the nonlinearity of air as a significant contribution to the total nonlinearity in a thin disk laser cavity. Flooding the laser cavity with helium has allowed us to eliminate this contribution and to decrease the repetition rate to 12.3 MHz. The current result is limited by the available pump power and optics for a further increase of the cavity length. We therefore believe that a further increase of the pulse energy is possible, e.g., by using a multiple-pass cavity<sup>8,9,20</sup> to increase the cavity length while simplifying the setup and reducing the number of optics required.

## References

1. E. Innerhofer, T. Südmeyer, F. Brunner, R. Häring, A. Aschwanden, R. Paschotta, U. Keller, C. Hönninger, and M. Kumkar, *Opt. Lett.* **28**, 367 (2003).
2. F. Brunner, E. Innerhofer, S. V. Marchese, T. Südmeyer, R. Paschotta, T. Usami, H. Ito, S. Kurimura, K. Kitamura, G. Arisholm, and U. Keller, *Opt. Lett.* **29**, 1921 (2004).
3. T. Südmeyer, J. Aus der Au, R. Paschotta, U. Keller, P. G. R. Smith, G. W. Ross, and D. C. Hanna, *Opt. Lett.* **26**, 304 (2001).
4. T. Südmeyer, E. Innerhofer, F. Brunner, R. Paschotta, U. Keller, T. Usami, H. Ito, M. Nakamura, K. Kitamura, and D. C. Hanna, *Opt. Lett.* **29**, 1111 (2004).
5. T. Südmeyer, J. Aus der Au, R. Paschotta, U. Keller, P. G. R. Smith, G. W. Ross, and D. C. Hanna, *J. Phys. D* **34**, 2433 (2001).
6. S. V. Marchese, E. Innerhofer, R. Paschotta, S. Kurimura, K. Kitamura, G. Arisholm, and U. Keller, *Appl. Phys. B* **81**, 1049 (2005).
7. F. Röser, J. Rothhard, B. Ortac, A. Liem, O. Schmidt, T. Schreiber, J. Limpert, and A. Tünnermann, *Opt. Lett.* **30**, 2754 (2005).
8. S. H. Cho, B. E. Bouma, E. P. Ippen, and J. G. Fujimoto, *Opt. Lett.* **24**, 417 (1999).
9. S. Naumov, A. Fernandez, R. Graf, P. Dombi, F. Krausz, and A. Apolonski, *New J. Phys.* **7**, 216 (2005).
10. S. Dewald, M. Siegel, R. Moshhammer, and U. Morgner, in *Conference on Lasers and Electro-Optics* (Optical Society of America, 2006), paper CMG 1.
11. A. Killi, A. Steinmann, J. Dörring, U. Morgner, M. J. Lederer, D. Kopf, and C. Fallnich, *Opt. Lett.* **30**, 1891 (2005).
12. A. Giesen, H. Hügel, A. Voss, K. Wittig, U. Brauch, and H. Opower, *Appl. Phys. B* **58**, 365 (1994).
13. U. Keller, D. A. B. Miller, G. D. Boyd, T. H. Chiu, J. F. Ferguson, and M. T. Asom, *Opt. Lett.* **17**, 505 (1992).
14. U. Keller, K. J. Weingarten, F. X. Kärtner, D. Kopf, B. Braun, I. D. Jung, R. Fluck, C. Hönninger, N. Matuschek, and J. Aus der Au, *IEEE J. Sel. Top. Quantum Electron.* **2**, 435 (1996).
15. F. X. Kärtner and U. Keller, *Opt. Lett.* **20**, 16 (1995).
16. J. Aus der Au, G. J. Spühler, T. Südmeyer, R. Paschotta, R. Hövel, M. Moser, S. Erhard, M. Karszewski, A. Giesen, and U. Keller, *Opt. Lett.* **25**, 859 (2000).
17. A. Tünnermann, H. Zellmer, W. Schöne, A. Giesen, and K. Contag, in *High-Power Diode Lasers*, R. Diehl, ed., Vol. 78 of *Topics in Applied Physics* (Springer-Verlag, 2000), p. 369.
18. R. Paschotta and U. Keller, *Appl. Phys. B* **73**, 653 (2001).
19. E. T. J. Nibbering, G. Grillon, M. A. Franco, B. S. Prade, and A. Mysyrowicz, *J. Opt. Soc. Am. B* **14**, 650 (1997).
20. D. Herriott, H. Kogelnik, and R. Kompfner, *Appl. Opt.* **3**, 523 (1964).